An Investigation of the Detonation Jetting Phenomenon

Rachel Hytovick, Robert Burke, Taha Rezzag, Kareem Ahmed
University of Central Florida
Orlando, Florida, USA

1 Introduction

The rotating and pulse detonation engines (RDE and PDE) have the potential to enhance thermodynamic cycles [1, 2]. Detonations provide increased thermodynamics efficiencies and higher levels of heat release with less required fuel when compared to traditional gas turbine engines [3]. Only after several decades of comprehensive rotating detonation studies have they become a reality in new-generation engines [4]. Today, RDE research pushes towards using jet fuels for rotating detonation engines, thus requiring a further understanding of the jet fuel detonation process [5].

Several studies have been conducted to achieve a larger understanding of the instabilities that occur within the detonation front and structure [6], in which the general cell structure has been thoroughly defined [7]. In weak detonations, there is a continuous cycle of transverse waves intersecting with an incident shock and Mach stem, forming a triple point [8]. Additionally, transverse waves collide both at and behind the detonation front[8]. Some studies have postulated that a highly reactive area forms at these transverse wave intersections [9, 10]. In this small-scale, high-energy area where two transverse waves coalesce, a jetting phenomenon develops, occurring frequently during propagation [11]. The jets produced at this coalescence likely attribute to the steady propagation of the unstable detonation fronts maintained through various instabilities [12]. However, this jetting phenomenon occurs in very localized areas, making the jet difficult to observe and understand.

Additionally, while many of these studies have focused simple gaseous fuel mixtures, it has been generally assumed that jet fuel driven detonations propagate similarly, undergoing the same phenomenon. However, many liquid-based detonation engines have experimentally shown significant velocity deficits when compared to theoretical values [13, 14]. This has led to an increased need in understanding liquid detonation propagation and determination of the burning conditions of vaporized liquids.

This work presents experimental results of the detonation jetting phenomenon for both liquid jet fuels and gaseous mixtures. Using stoichiometric hydrogen-air detonation for a benchmark, previously theorized and computational jetting dynamics are witnessed. In addition, two vaporized liquid fuel mixtures (RP-2 and JP-10 oxygen) are investigated. This study used a combination of ultra-high-speed schlieren, chemiluminescence, and pressure measurements to study the effect of the localized jetting phenomenon both quantitatively and qualitatively.

2 Methodology

2.1 Facility Overview

A detonation facility was used with two different filling schemes for the fuels (gaseous and liquid-based fuels). The stainless steel facility, shown in Figure 1, has a 45 x 45 mm^2 cross-section. The mixture is adjustable at the injection plenum, followed by a 0.68 m removable turbulence generator. While in
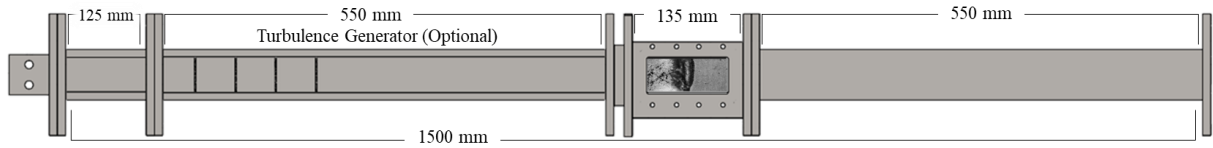
Figure 1: Facility Overview

place, the turbulence generator consists of five closely positioned perforated plates followed by a sixth plate prior to the test section. The test section provides 101.6 x 45 mm^2 of optical access via two 25 mm thick fused silica windows.

Following reactant mixture injection, the experiments begin with weak ignition via a spark plug. The resulting flame front propagates through the channel and begins to accelerate. Eventually, the mixture reaches the speed of sound of the reactants, forming a normal shock. Following this event, the flame undergoes self-compression leading to more acceleration and eventually a detonation.

2.2 Diagnostics

For this experiment, ultra-high-speed schlieren, CH* chemiluminescence, and pressure measurements are recorded. Schlieren was captured in the conventional z-setup while the chemiluminescence was collected at a slight angle near the test section. The ultra-high-speed schlieren was collected with a Shimadzu camera recording between 1 and 5 MHz. This measurement was captured at varying fields of view (FOV), ranging between 25 x 15 mm^2 and 60 x 45 mm^2. The Shimadzu data were obtained at a fixed resolution of 400 x 250 pixels. With the varying FOV, the pixel-based uncertainty lies between 10 and 26 m/s depending on the test case parameters.

Broadband and CH* chemiluminescence, for hydrogen and hydrocarbons respectively, was captured with a Photron Fastcam SA-Z. The chemiluminescence was captured at 400 kHz with a resolution of 128 x 104 pixels. The data for this measurement was recorded at a 7.4-degree angle off the line-of-sight view and targeted the second half of the test section, roughly 60 x 45 mm^2. This diagnostic was used to track the detonation front and ensure ignition of the hydrocarbons in the hydrocarbon-hydrogen fuel blends.

Finally, five high-speed piezoelectric pressure transducers recorded pressure measurements leading up to and throughout the test section. These measurements were collected at 1 MHz, offering significant insight into detonation jetting behavior. They also allowed for precision timing when triggering the other diagnostics.

2.3 Injection Schematic

This experiment tested both liquid-based and gaseous fuel mixtures. The injection method for the different mixtures varied significantly and are expanded upon below.

2.3.1 Gaseous Mixtures

The gaseous mixture used in this experiment was a stoichiometric hydrogen-air mixture. The facility has been used to study hydrogen-air mixtures and this injection method is further expanded upon in various other works [15-17]. An overview of this injection method is shown in Figure 2a. For hydrogen-air mixtures, pressure is regulated at the compressed gas cylinders. The
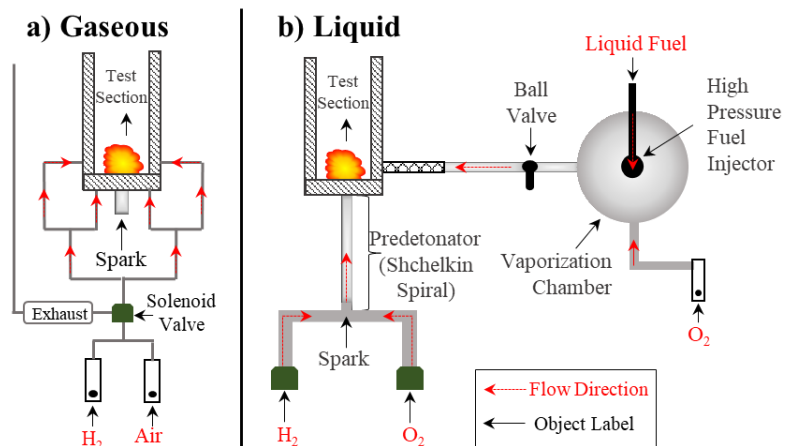

Figure 2: Injection Schematics

flow rates are controlled through Dwyer VFA flow meters. The inflow is pre-mixed. The eight tubes are then injected into the beginning of the facility. The mixture fills the facility for 20 seconds, entirely consuming its volume before it is ignited. At ignition, a solenoid valve is triggered to exhaust the facility, preventing backpressure. The flame then propagates through the channel as described above.

2.3.2 Liquid Mixtures

Both RP-2 and JP-10 liquid fuel mixtures were also tested. An overview of this injection method is shown in Figure 2b. For these tests, fueling began by filling a mixing chamber with oxygen. The mixture chamber then is closed as liquid aerosolized injection begins. The fuel injector (Continental XL3 GDI), positioned at the top of the cylindrical channel, was pressurized to 2500 psi to ensure atomization of the liquid fuel into the chamber. This high-pressure injection approach generates fuel droplets below 1 micron which are then evaporated within the chamber. The injection was controlled through a pulse/delay generator, which was set for a pulse width of 0.38 ms, passing 3.047 mg of fuel per pulse. For this experiment, detonability was optimized at 310 pulses, for both RP-2 and JP-10. After the injection was complete, the mixture was filled into the facility for another 10 seconds. Once the facility was consumed, a hydrogen-oxygen pre-detonator was ignited. This provided a slightly stronger ignition source to promote heating and mixing of the vaporized hydrocarbons. Hydrocarbon ignition was
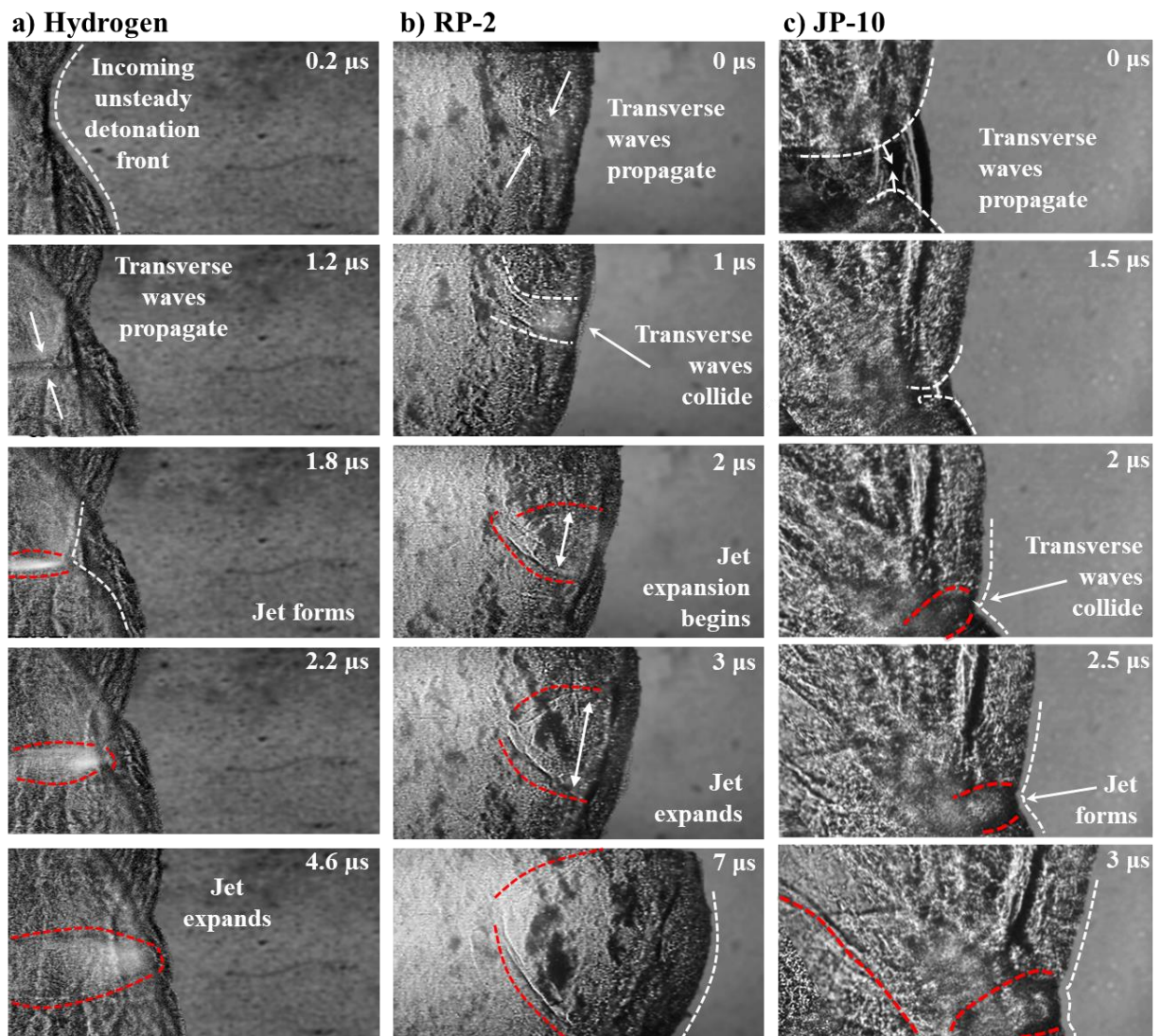

Figure 3: Jetting Evolution for Various Fuels

confirmed through CH* chemiluminescence. For the liquid cases in this experiment, the turbulence generators were removed.

3   Results and Discussion

The dynamics of the detonation jetting phenomenon were captured experimentally and are presented for hydrogen, RP-2, and JP-10 fuel mixtures in Figure 4a, b, and c. Figure 4a displays a hydrogen jet forming at the interaction of two transverse waves. This test case was captured with a 60 x 45 mm field of view at 5 MHz. As the detonation front enters the frame, it does not have the typical planar front and is assumed to be restructuring. Initially, at 0.2 µs, three fronts are visible. After 1 microsecond, two dominating transverse waves appear on the same plane. Within the next microsecond, these transverse waves collide and form an area of high energy release, visualized by the oversaturation witnessed in the third and fourth frames. Following this, the jet expands and overcomes the front, eventually creating a planar detonation front. Assuming a 15 mm cell size for a stoichiometric hydrogen-air case, it is possible to witness three detonation cells in this window [6]. The 4.6 µs that is captured of the detonation front reveals the largely theoretical process of the jetting that forms at the triple point of the transverse waves [11].

Figure 4b and c, show the same process for RP-2 and JP-10 mixtures. The RP-2 case, shown in Figure 4b, is captured 1 MHz. The process of transverse waves coalescing to form a jet remains evident. In this case, the jet appears to consume more of the field of view. This is likely due to the increased detonation cell size in comparison to hydrogen [14]. It is also notable that the jet appears to be more circular than elliptical. In the final image set, Figure 4c, a JP-10 mixture is examined over 3 µs. This mixture is investigated over a much smaller region, 23.5 x 14.7 mm at a frame rate of 2 MHz. In this data set, the propagation of transverse waves on the same plane is highly visible. Both the transverse waves front and propagating material directly behind it can be seen traveling inwards. These images also reveal the initial energy release of the jet. In the third image, the previously visible background shock becomes consumed from the radially expanding jet. In the next half microsecond, the jet overtakes the detonation front and begins to expand as seen prior in other fuels.

While Figure 3a-c demonstrates the visual features of the jetting phenomenon captured in both liquid and gaseous mixtures, Figure 4a and b provide quantitative measurements of the detonations. The dotted gray lines in each plot signify the theoretical Chapman-
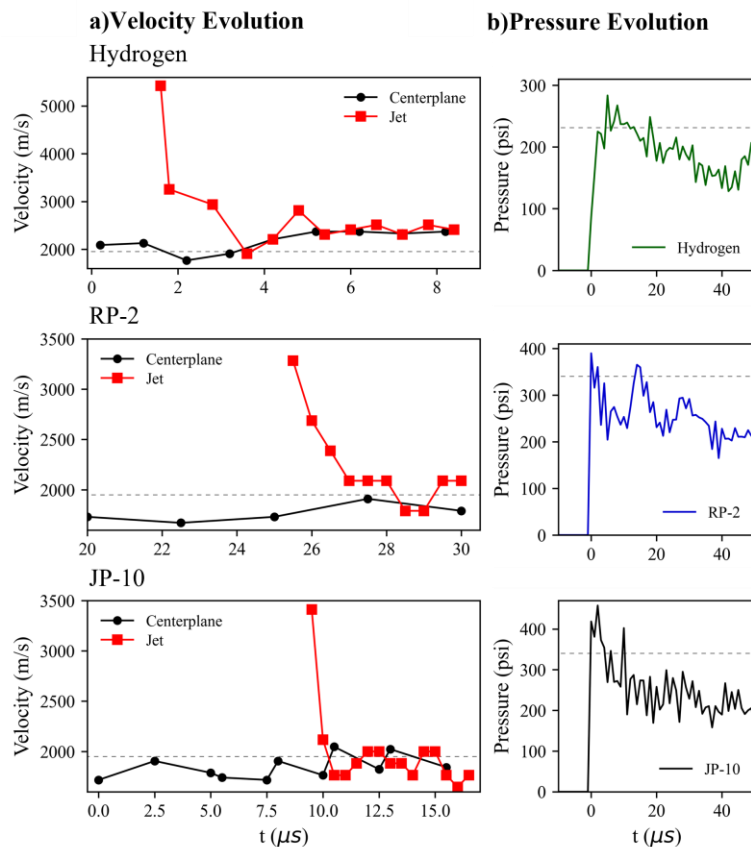

Figure 4: Velocity and Pressure Traces

Jouguet values for that mixture and parameter. The corresponding values for each fuel are tabulated in Table 1.

In Figure 4a, the velocity evolutions are shown for the discussed mixtures. The velocities were collected at three locations in the vertical direction for each frame and then averaged over each frame for accuracy. All mixtures propagate around their theoretical velocities. The instabilities and variances shown are attributed to the detonation cell cycle fluctuations that are captured when recording data over 1 MHz. Regarding the detonation jetting velocities, the first velocity is recorded at the first notable outward expansion of the jetting phenomenon. The velocity is then collected at the jet front until the wave exits the field of view. In Figure 4b, pressure evolutions are resolved. It is noted that like velocity, all three wavefronts are meeting and slightly exceed the respective theoretical CJ parameters.

In Table 1, the measured values for each parameter are noted. For the RP-2 and JP-10 mixtures, it should be considered that they contained trace amounts of hydrogen in the mixture due to the injection scheme. These trace amounts are attributed to a slight increase in theoretical parameters. Additionally, the continued similarities between the liquid fuels are expected. The fuels are both regarded as heavier hydrocarbons and have very similar lower heating values (44 MJ/kg for RP-2 and 43.8 MJ/kg for JP-10) that consequently lead to analogous levels of heat and energy release[18, 19]. This experiment allowed the stoichiometric hydrogen-air mixture to stand as a well-characterized benchmark while highlighting both expected and unexpected findings in the vaporized liquid mixtures.

Table 1: Tabulated Quantitative Results

Fuel	*Oxidizer*	$U_{front,\ avg}$ *(m/s)*	$U_{front,avg}/U_{CJ}$	U_{jet} *(m/s)*	P_{max} *(psi)*	P_{max}/P_{CJ}
H_2	*Air*	*2071*	*1.02*	*5422*	*289*	*1.23*
JP-10	O_2	*1976*	*1.02*	*3411*	*402*	*1.18*
RP-2	O_2	*1912*	*0.99*	*3238*	*394*	*1.16*

4   Conclusion

Ultimately, this work provided support and insight into the driving instabilities that occur on a detonation front via experimental investigation of various fuels in varying states. It revealed the reasonable differences and similarities when using hydrocarbon liquids instead of hydrogen gas mixtures. This work contributes to the broader understanding of an intrinsically unstable combustion process. Through these advances, improved technology can be implemented into next-generation propulsion devices. Additionally, through an improved understanding of the driving mechanisms behind detonations, further improvements in the scientific understanding of astrophysical combustion can be attained.

Acknowledgements

References

[1]   G. D. Roy, S. M. Frolov, A. A. Borisov, and D. W. Netzer, "Pulse detonation propulsion: challenges, current status, and future perspective," *Progress in Energy and Combustion Science,* vol. 30, no. 6, pp. 545-672, 2004.

[2]   J. C. Leyer, A. A. Borisov, W. A. Sirignano, and A. L. Kuhl, *Dynamics of Heterogeneous Combustion and Reacting Systems*. 1993.

[3]   Y. B. Zeldovich, "To the Question of Energy Use of Detonation Combustion," *Journal of Propulsion and Power,* vol. 22, no. 3, pp. 588-592, 2006.

[4]   T. Sato and V. Raman, "Detonation Structure in Ethylene/Air-Based Non-Premixed Rotating Detonation Engine," *Journal of Propulsion and Power,* vol. 36, no. 5, pp. 752-762, 2020.

[5]   W. A. Hargus, S. A. Schumaker, and E. J. Paulson, "Air Force Research Laboratory Rotating Detonation Rocket Engine Development," presented at the 2018 Joint Propulsion Conference, 2018.

[6]   P. Clavin and F. A. Williams, "Analytical studies of the dynamics of gaseous detonations," *Philos Trans A Math Phys Eng Sci,* vol. 370, no. 1960, pp. 597-624, Feb 13 2012.

[7]   M. I. Radulescu, G. J. Sharpe, C. K. Law, and J. H. S. Lee, "The hydrodynamic structure of unstable cellular detonations," *Journal of Fluid Mechanics,* vol. 580, pp. 31-81, 2007.

[8]   V. N. Gamezo, A. Y. Poludnenko, E. S. Oran, and F. A. Williams, "Transverse waves resulting from pulsating instability of two-dimensional flames," *Combustion and Flame,* vol. 161, no. 4, pp. 950-957, 2014.

[9]   S. S. M. Lau-Chapdelaine, Q. Xiao, and M. I. Radulescu, "Viscous jetting and Mach stem bifurcation in shock reflections: experiments and simulations," *Journal of Fluid Mechanics,* vol. 908, 2020.

[10]   B. Edney, "ANOMALOUS HEAT TRANSFER AND PRESSURE DISTRIBUTIONS ON BLUNT BODIES AT HYPERSONIC SPEEDS IN THE PRESENCE OF AN IMPINGING SHOCK," Office of Scientific and Technical Information (OSTI)1968, Available: https://dx.doi.org/10.2172/4480948.

[11]   S. R. Sanderson, J. M. Austin, Z. Liang, F. Pintgen, J. E. Shepherd, and H. G. Hornung, "Reactant jetting in unstable detonation," *Progress in Aerospace Sciences,* vol. 46, no. 2-3, pp. 116-131, 2010.

[12]   C. Ruan, F. Chen, W. Cai, Y. Qian, L. Yu, and X. Lu, "Principles of non-intrusive diagnostic techniques and their applications for fundamental studies of combustion instabilities in gas turbine combustors: A brief review," *Aerospace Science and Technology,* vol. 84, pp. 585-603, 2019.

[13]   J. Kindracki, "Experimental research on rotating detonation in liquid fuel–gaseous air mixtures," *Aerospace Science and Technology,* vol. 43, pp. 445-453, 2015.

[14]   R. Akbar, "Detonation Properties of Sensetized and Unsensitized JP-10 and Jet-A Fuels in Air for Pulse Detonation Engines," *Joint Propulsion Conference,* Conference vol. 36, 2000 2000.

[15]   R. Hytovick, H. M. Chin, and K. A. Ahmed, "Investigation of Controlled Deflagration-to-Detonation Transition of Hydrocarbon Fuels," presented at the AIAA Scitech 2021 Forum, 2021.

[16]   H. M. Chin, J. Chambers, J. Sosa, and K. A. Ahmed, "Quantification of Pressure Gain in Turbulent Fast Flames for Deflagration-to-Detonation," presented at the AIAA Scitech 2020 Forum, 2020.

[17]   J. Sosa, J. Chambers, K. A. Ahmed, A. Poludnenko, and V. N. Gamezo, "Compressible turbulent flame speeds of highly turbulent standing flames," *Proceedings of the Combustion Institute,* vol. 37, no. 3, pp. 3495-3502, 2019.

[18]   H. Wang *et al.*, "A physics-based approach to modeling real-fuel combustion chemistry - I. Evidence from experiments, and thermodynamic, chemical kinetic and statistical considerations," *Combustion and Flame,* vol. 193, pp. 502-519, 2018.

[19]   R. Xu and H. Wang, "Principle of large component number in multicomponent fuel combustion – a Monte Carlo study," *Proceedings of the Combustion Institute,* vol. 37, no. 1, pp. 613-620, 2019.